CHEMICAL ENGINEERING TRANSACTIONS
VOL. 41, 2014
A publication of AIDIC
The Italian Association of Chemical Engineering
www.aidic.it/cet
Guest Editors: Simonetta Palmas, Michele Mascia, Annalisa Vacca

ISBN 978-88-95608-32-7; **ISSN** 2283-9216
DOI: 10.3303/CET1441001

The 3D Printing of a Polymeric Electrochemical Cell Body and its Characterisation

C. Ponce de Leon[a]*, W. Hussey[a], F. Frazao[a], D. Jones[a], E. Ruggeri[a], S. Tzortzatos[a], R.D. Mckerracher[a], R.G.A. Wills[a], S. Yang[b], F.C. Walsh[a, b]

[a] Electrochemical Engineering Laboratory, Energy Technology Research Group, University of Southampton, Highfield, Southampton, SO17 1BJ, UK
[b]Engineering Materials Research Group, Engineering Sciences, University of Southampton, Highfield, Southampton, SO17 1BJ, UK
capla@soton.ac.uk

An undivided flow cell was designed and constructed using additive manufacturing technology and its mass transport characteristics were evaluated using the reduction of ferricyanide, hexacyanoferrate (III) ions at a nickel surface. The dimensionless mass transfer correlation $Sh = aRe^{b}Sc^{d}Le^{e}$ was obtained using the convective-diffusion limiting current observed in linear sweep voltammetry; this correlation compared closely with that reported in the literature from traditionally machined plane parallel rectangular flow channel reactors. The ability of 3D printer technology, aided by computational graphics, to rapidly and conveniently design, manufacture and re-design the geometrical characteristics of the flow cell is highlighted.

1. Introduction

Rapid prototype shaping of solid materials has classically been limited to heavy duty CNC (computer numerical control) machinery, typically mills and lathes. The gradual introduction of affordable 3D printers over the last decade, however, has revolutionized this process. Additive manufacturing or 3D printing technology allows the production of intricate designs that would otherwise require longer and complex manufacturing processes while reducing manufacturing cost and material waste (Czyżewski et al., 2009), e.g. single blocks containing internal channels and manifolds.
Typical 3D printers operate by selective deposition of material as filaments on a base, or by selectively binding the material together with a laser, layer by layer (Critchley et al., 2013, Lipson et al., 2013 and Pham and Gault, 1998). Complex designs such as auxetic foams can be easily generated and altered whenever necessary. The advantages are fast, automated manufacturing, low cost, recyclability of material, a low number of manufacturing processes and tools, readily available raw materials, higher portability and easy implementation of design alterations. Some limitations include the potential loss in accuracy, and the presence of residual stresses that might deform and change mechanical properties of the final component. While simple 3D printers have become available at moderate cost, high capital investment is required for sophisticated, high precision, multi-material, multiple printing head devices (Vaezi et al., 2013a, Rankin et al., 2014 and Lemu 2012).
Fuel cells and redox flow batteries are currently manufactured on a one-by-one basis due to the large number of parts involved in their production, and are integrated in a single module which needs to have careful alignment of parts. The process is labour intensive and requires skilled workshop techniques such as cutting, milling and drilling. Redesigns (which often occur following early evaluation) are tedious and costly in terms of labour, materials and time. The flexibility offered by 3D printing could be used to produce complex flow cell designs which are sized and profiled and potentially realised in a single, facile process, reducing the amount of material, labour and cost. This technology has already been used in several applications such as the manufacture of a 10-cell air-breathing miniature PEMFC stack that operated with 99.999 % hydrogen at maximum power of 99 mW cm^{-2} at 0.425 V connected in series at 70 ^{o}C (Chen et

Please cite this article as: Ponce De Leon C., Hussey W. , Frazao F., Jones D., Ruggeri E., Tzortzatos S., Mckerracher R., Wills R.G.A., Yangb S., Walsh F., 2014, The 3d printing of a polymeric electrochemical cell body and its characterisation, Chemical Engineering Transactions, 41, 1-6 DOI: 10.3303/CET1441001

al., 2008). Chen et al., (2010) used additive manufacturing to manufacture a honeycomb shaped reservoir and a flow distributor for a direct methanol, fuel cell that would have been very difficult to produce via traditional manufacturing technology. Additive manufacturing has also been used in combination with thermal spray to produce the bipolar plates (Lyons et al., 2005). The authors report that the metallic part meets the requirements of a PEMFC using minimum materials and processing cost. Porous carbons (Lu et al., 2012) and body implants (Moroni et al., 2008), together with a number of other applications, have been reported (Vaezi et al., 2013b).

Most of the applications of rapid prototyping in electrochemistry to date have been limited to small scale fuel cell prototypes. In this paper we report the manufacture and mass transport characterisation of a larger undivided flow cell (49 cm^2 electrode area) that can be used for a variety of laboratory and pilot-scale electrochemical experiments such as redox flow cells, corrosion and electrodeposition, metal ion removal, organic oxidation of wastes and electrochemical synthesis. The mass transport characteristics of the 3D printed cell were characterised by the conventional $K_4Fe(CN)_6/K_3Fe(CN)_6$ redox couple and compared with existing flow cells manufactured via traditional machining..

2. Experimental details

The cell was first conceived in the SolidWorks CAD software and converted into a .stl digital format suitable for input to the 3D printer. The electrolyte channel was manufactured using a selective deposition printer UP! 2 Plus (by PP3DP) while, for the endplates, an Ultra® 3SP (by Envision TEC) allowing more accurate manufacture, a higher quality surface finish and better mechanical properties, was preferred (Lipson et al., 2013, Vaezi et al., 2013a, Rankin et al., 2014, Lemu et al., 2012).

The material used to manufacture the undivided electrochemical flow cell was ABS (acrylonitrile butadiene styrene) polymer and comprised a central flow compartment of 10 length × 8.5 cm width and 1.4 cm thickness held together with two 1.4 cm thick endplates of 16.5 cm length × 12.5 cm width, the assembly being compressed with 10 M6 stainless steel tie-bolts. The middle compartment had a square, 7 × 7 cm void space in the centre that formed the electrolyte channel, providing an exposed electrode area of 49 cm^2. Nickel foil of 0.1 mm thickness and 99.9% wt. purity was used as the anode and cathode; silicone rubber gaskets were used between the compartments and the electrodes to seal the cell. Figures 1a) and 1b) show an expanded view of the flow cell and the electrolyte flow circuit, respectively. A Luggin capillary tube of was inserted at the exit manifold in order to measure the electrode potentials against an Ag/AgCl reference electrode. The composition of the electrolyte was 1 mmol dm^{-3} $K_3Fe(CN)_6$ and 10 mmol dm^{-3} $K_4Fe(CN)_6$ in 1 mol dm^{-3} Na_2CO_3. The selection of Na_2CO_3 was based on previous works that suggest that this electrolyte provides a more reliable limiting current (Taama et al., 1996, Szánto et al., 2008). The flow circuit included a Totton EMP40/4 centrifuge pump and a calibrated flowmeter with a PVDF float with a range between 0 – 100 dm^3 h^{-1} and a by-pass to control the flow rate. The solutions were used immediately after preparation to minimise the effects of the degradation of the electrolyte in the measured current. Table 1 shows the characteristics of the flow cell and the electrolyte.

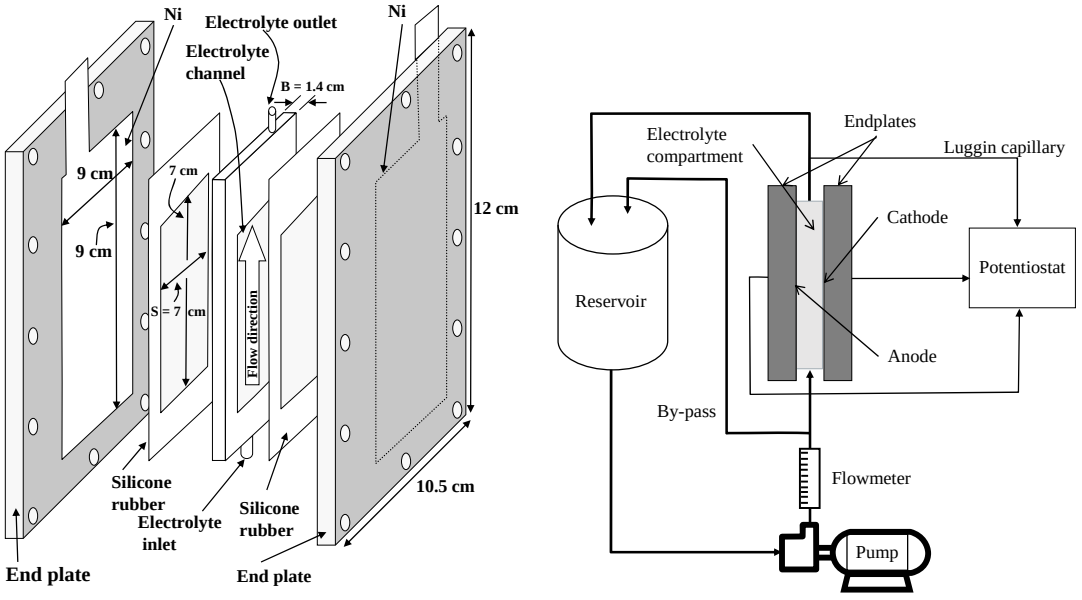

Figure 1 a) Expanded view of the 3D printed cell. Not to scale. b) electrolyte flow circuit.

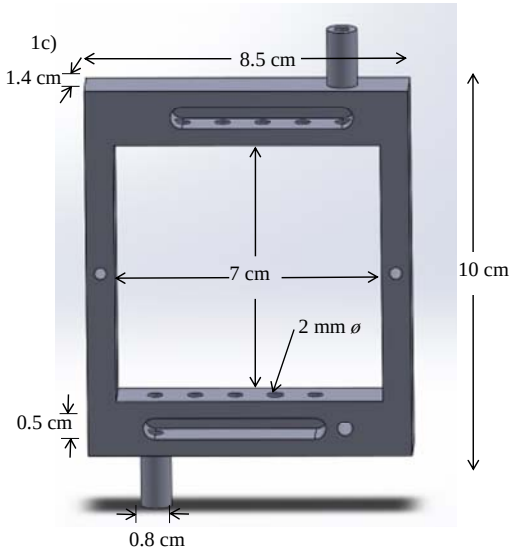

Figure 1c) SolidWorks digital image of the 3D cell.

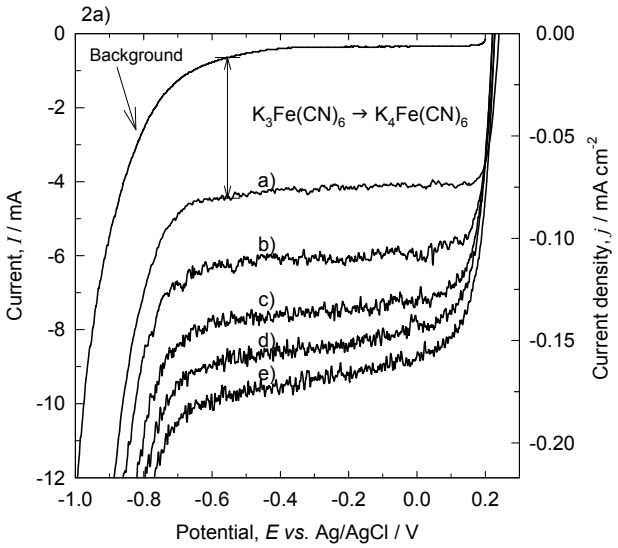

Figure 2a) Reduction of ferricyanide ions in a solution containing 1 mmol dm^{-3} $K_3Fe(CN)_6$ + 10 mmol dm^{-3} $K_4Fe(CN)_6$ in 1 mol dm^{-3} Na_2CO_3 at Ni electrodes of 49 cm^2 geometrical area at a potential sweep rate of 5 mV s^{-1}.

3. Results and Discussion

Figure 2a shows linear sweep voltammetry curves for reduction of ferricyanide ions on a flat plate nickel electrode at a potential sweep rate of 5 mV s^{-1} at different flow rates. The cyclic voltammetry curves show the characteristic shape with kinetic, mixed and mass transport controlled regions together with the secondary reaction of hydrogen evolution. The mass transport controlled region between 0 V and -0.6 V *vs*. Ag/AgCl was used to calculate the limiting current values. Figure 2b shows the current *vs*. time curves when a potential of -0.4 V *vs*. Ag/AgCl in the limiting current region was applied and the flow rate of the electrolyte was changed. One of the curves in the Figure 2b shows the value of the current when a turbulence promoter of a 30 pores per linear inch (ppi) polyester foam (cell diameter 1.6-1.9 mm from Sydney Heath & Son Ltd) fitted inside the electrolyte compartment. The graph shows that the turbulence promoter helps to increase the limiting current from 15 % at the lowest flow rate up to 31% at the highest flow rate. The limiting current values obtained from the linear sweep voltammetry and chronopotentiometry can be used to calculate the steady state mass transfer coefficient associated to the electrode area k_LA from the equation:

$$k_L A = \frac{I_L}{nF\Delta c} \tag{1}$$

where *n*, *F* and *c* are the number of electrons interchanged, the Faraday constant and the bulk concentration of ferricyanide ion. The k_LA values, together with the parameters of Table 1, were used to calculate the dimensionless numbers *Sh*, *Re*, *Sc* and *Le* in order to establish the mass transport relationship (Pickett, 1979):

$$Sh = aRe^bSc^dLe^e \tag{2}$$

Figure 3 shows the Sherwood number *vs*. Reynolds number correlations for a number of parallel plate configuration cells taken from the literature such as the FM01-LC laboratory electrolyser (Brown et al., 1993, Griffiths et al., 2005) and the ElectroSynCell (Carlsson et al., 1983) compared with the data obtained with the 3D printed cell. The literature indicates that the data presented in the plots was obtained using nickel electrodes or electrodeposited nanostructured nickel surfaces of high surface area (Recio et al., 2013) in order to evaluate the mass transport relationships. The figure also shows the curves for fully developed laminar flow with a relationship: *Sh* = 1.85γ (*Re Sc Le*) 0.33 (*γ* is a geometrical correction factor) and for fully developed turbulent flow, $Sh = 0.45Re^{0.66}Sc^{0.33}Le^{0.25}$ (Pickett, 1979) in an empty rectangular channel. The data obtained using the 3D printed cell compare favourably to the other electrochemical reactors in the 150 < *Re* < 800 range studied. At these Reynolds numbers, the laminar

flow is expected with a Re exponent of 0.33, but the data for the 3D printer shows a *Sh vs. Re* relationship $Sh = 1.22Re^{0.65}Sc^{0.33}Le^{0.25}$ which indicates turbulent flow as the Reynolds number exponent is 0.65. This is attributable to the absence of a calming zone that allows the flow fluid to develop into laminar flow when the electrolyte enters the compartment the 3D printed cell.

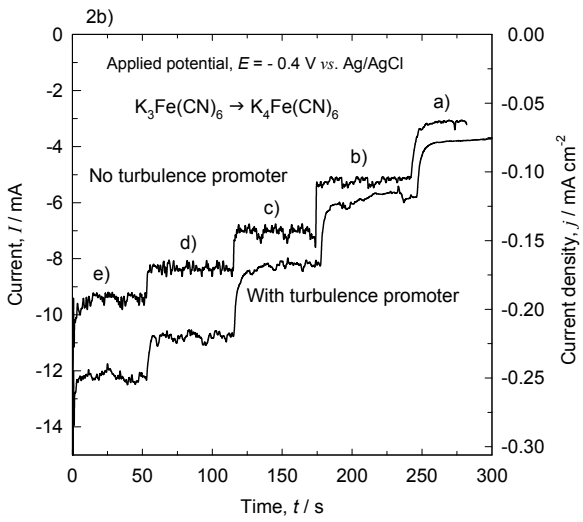

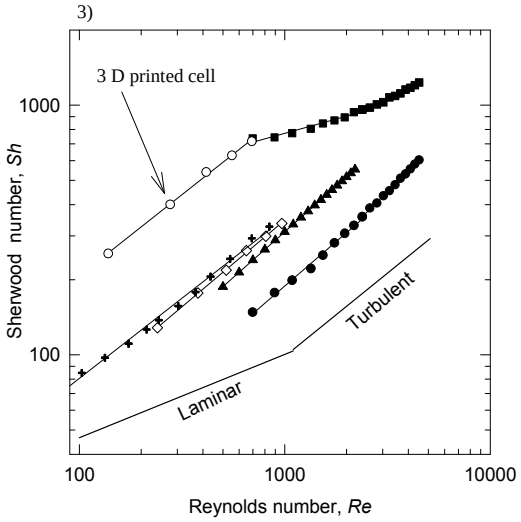

Figure 2b) current vs. time curves for the reduction of ferricyanide ions in a solution containing 1 mmol dm^{-3} $K_3Fe(CN)_6$ + 10 mmol dm^{-3} $K_4Fe(CN)_6$ in 1 mol dm^{-3} Na_2CO_3 at nickel electrodes of 49 cm^2 geometrical area at -0.4 V vs. Ag/AgCl. Flow rates: a) 20, b) 40, c) 60 d) 80 and d) 100 dm^3 h^{-1}.

Figure 3) l*og-log plot of Sh vs. Re for various rectangular flow channel cells containing nickel electrodes. The solid lines show fully developed laminar and turbulent flow relationships in an empty rectangular channel (Pickett, 1979). ○) Ni in a 3D printed flow cell, ◇) and ▲) Ni in the FM01-LC electrolyser (Brown et al., 1993, Griffiths et al., 2005), +) Ni in the ElectroSynCell (Carlsson et al., 1983), ●) solid Ni and ■) nanostructured Ni electrodeposit (Recio et al., 2013).*

Table 1: Dimensions of the flow cell and characteristics of the electrolyte

Characteristic	Values
Electrode width, *B*	7 cm
Electrode spacing, *S*	1.4 cm
Electrode geometric area, *A* = *BL*	49 cm^2
Equivalent diameter of flow channel, $d_e = 2BS/(B+S)$	2.33 cm
Length of the electrolyte compartment, *L*	7 cm
Kinematic viscosity of electrolyte, *v*	9.56 x 10^{-3} cm^2 s^{-1}
Diffusion coefficient of $Fe(CN)_6^{-3}$, *D*	6.4 x 10^{-6} cm^2 s^{-1}
Density of the electrolyte, ρ	1.0985 g cm^{-3}
Sh	$k_L de/D$
Re	ude/ν
Schmidt number, *Sc*	1494
Dimensionless length, $L_e = d_e/L$	0.125
Electrolyte composition	1 x 10^{-3} mol dm^{-3} $K_3Fe(CN)_6$ + 10 x 10^{-3} mol dm^{-3} $K_4Fe(CN)_6$ + 1 mol dm^{-3} Na_2CO_3
Mean linear electrolyte flow velocity, *u*	0.5 to 3.0 cm s^{-1}
Temperature	302 K

Additive manufacturing can be used to modify and manufacture an improved 3D printed flow cell, to include a calm zone and better flow distributors. Although this can be done very quickly, other factors should be taken into account such as: 1) heat deformation of the components due to residual stress caused by the high temperature of the newly deposited layers and 2) the resolution of the 3D printer machine, which will have a direct impact on the porosity of the components and can cause leakage of the electrolyte. These aspects can be resolved by careful choice of additive manufacturing technology and the materials for printing. Despite these disadvantages, additive manufacturing technology is evolving very fast and offers great opportunity to manufacture complex more efficient and high space time yield electrochemical reactors. The process to achieve an ideal flow cell might typically involve several iterations, following feedback from experimental results.

4. Conclusions

The 3D printed cell showed turbulent flow at low Reynolds numbers due to the geometry of the electrolyte channel. Additional cells can be readily manufactured using 3D printing technologies informed by process experience from previous results. 3D printing technology is still evolving rapidly and electrochemical cells design can benefit from this technology: flow cells can be designed and constructed in a single day, a complete electrolyte compartment with a built in turbulence promoter can be manufactured. The 3D printed flow cell operates well and its global mass transport behaviour is comparable to traditional flow cells.

Acknowledgements

Parts of the reported studies were pursued via an MEng final year undergraduate group design project in engineering by W.H., F.F., D.J., E.R. and S.T, October, 2013 to May, 2014.

References

Brown C.J., Pletcher D., Walsh F.C., Hammond J.K., Robinson D., 1993, Studies of space-averaged mass transport in the FM01-LC laboratory electrolyser, Journal of Applied Electrochemistry, 23, 38-43, DOI: 10.1007/BF00241573

Carlsson I., Sandegren B., Simonsson D, 1983, Design And Performance Of A Modular, Multi-Purpose Electrochemical Reactor, Journal of the Electrochemical Society, 130, 342-346, doi:10.1149/1.2119708

Chen C.Y., Lai W.H., Weng B.J., Chuang H.J., Hsieh C.Y., Kung C.C, 2008, Planar array stack design aided by rapid prototyping in development of air-breathing PEMFC, Journal of Power Sources, 179, 147-154, DOI: 10.1016/j.jpowsour.2007.12.080

Chen C.Y., Wen Y.C., Lai W.H., Chou M.C., Weng B.J., Hsieh C.Y., Kung C.C., 2010, A New Complex Design for Air-Breathing Polymer Electrolyte Membrane Fuel Cells Aided by Rapid Prototyping, J. Fuel Cell Sci. Technol 8, 014502-014502-4, DOI: 10.1115/1.4002227

Critchley R., Corni I., Wharton J.A., Walsh F.C., Wood R.J.K., Stokes K.R., 2013, A review of the manufacture mechanical properties and potential applications of auxetic foams, Physica Status Solidi B, 250, 1963-1982, DOI 10.1002/pssb.201248550

Czyżewski J., Burzyński P., Gawel K., and Maisner J., 2009, Rapid prototyping of electrically conductive components using 3D printing technology, Journal of Materials Processing Technology, 209, 5281-5285, DOI: 10.1016/j.jmatprotec.2009.03.015

Griffiths M., Ponce de Léon C., Walsh F.C., 2005, Mass transport in the rectangular channel of a filter-press electrolyzer (the FM01-LC reactor), AIChE Journal, 51, 682-687, DOI: 10.1002/aic.10311.

Lemu H.G., 2012, Study of capabilities and limitations of 3D printing technology, AIP Conf. Proc. 1431, 857-865, http://dx.doi.org/10.1063/1.4707644

Lipson H., Kurman M., 2013, Fabricated: The New World of 3D Printing, John Wiley & Sons, Indianapolis.

Lu X., Chen L., Amini N., Yang S., Evans J.R.G., Guo Z.X., 2012, Novel methods to fabricate macroporous 3D carbon scaffolds and ordered surface mesopores on carbon filaments, Journal of Porous Materials 19, 529-536, DOI: 10.1007/s10934-011-9501-x

Lyons B., Batalov M., Mohanty P., Das S., 2005, Rapid Prototyping of PEM Fuel Cell Bi-Polar Plates Using 3D Printing and Thermal Spray Deposition, Solid Freeform Fabrication Symposium Proceedings, 446-457.

Moroni L., Wijn J.R. de, Blitterswijk C.A. Van, 2008, Integrating novel technologies to fabricate smart scaffolds, Journal of Biomaterials Science, Polymer Edition, 19, 543-572, DOI: 10.1163/156856208784089571

Pham D.T., Gault R.S, 1998, A comparison of rapid prototyping technologies, International Journal of Machine Tools and Manufacture. 38, 1257-1287, DOI: 10.1016/S0890-6955(97)00137-5

Pickett D.J., 1979, Electrochemical Reactor Design, 2nd Edition, Elsevier, Amsterdam.
Rankin T.M., Giovinco N.A., Cucher D.J., Watts G., Hurwitz B., Armstrong D.G., 2014, Three-dimensional printing surgical instruments: are we there yet? Journal of Surgical Research, 189, 193-197, DOI:10.1016/j.jss.2014.02.020
Recio F.J., Herrasti P., Vazquez L., Ponce de León C., Walsh F.C., 2013, Mass transfer to a nanostructured nickel electrodeposit of high surface area in a rectangular flow channel, Electrochimica Acta 90, 507-513, DOI: 10.1016/j.electacta.2012.11.135
Szánto D.A., Cleghorn S., Ponce de León C., Walsh F.C., 2008, The limiting current for reduction of ferricyanide ion at nickel: The importance of experimental conditions, AIChE. Journal, 54, 802-810, DOI: 10.1002/aic.11420
Taama W.M., Plimley E.R., Scott K., 1996, Influence of supporting electrolyte on ferricyanide reduction at a rotating disc electrode Electrochimica. Acta, 41, 549-551, DOI: 10.1016/0013-4686(95)00390-8
Vaezi M., Chianrabutra S., Mellor B., Yang S., 2013a, Multiple material additive manufacturing – Part 1: a review, Virtual and Physical Prototyping, 8 19-50, DOI:10.1080/17452759.2013.778175
Vaezi M., Seitz H., Yang S., 2013b, A review on 3D micro-additive manufacturing technologies, The International Journal of Advanced Manufacturing Technology, 67, 1721-1754, DOI:10.1007/s00170-012-4605-2